PHILOSOPHICAL TRANSACTIONS OF THE ROYAL SOCIETY A MATHEMATICAL, PHYSICAL & ENGINEERING SCIENCES

The Composition of the Mesosphere and Lower Thermosphere

L. Thomas

Phil. Trans. R. Soc. Lond. A 1980 **296**, 243-260
doi: 10.1098/rsta.1980.0167

Phil. Trans. R. Soc. Lond. A **296**, 243–260 (1980) [243]
Printed in Great Britain

The composition of the mesosphere and lower thermosphere

By L. Thomas
Science Research Council, Appleton Laboratory, Ditton Park, Slough SL3 9JX, U.K.

The experimental information available on the neutral and ion composition of the 50–130 km height range is reviewed and, wherever possible, comparisons are made with predictions based on theoretical models.

The height distributions for various neutral constituents have been deduced from rocket-borne remote-sensing measurements and *in situ* sampling experiments, in which recent improvements in mass spectrometer techniques have been effective. The results obtained for oxygen, hydrogen, nitrogen and carbon species are described in turn. In addition, satellite-borne remote-sensing measurements have demonstrated the importance of temporal and spatial variations of molecular oxygen and nitric oxide in the lower thermosphere. *In situ* sampling with rocket-borne mass spectrometers has established that molecular oxygen and nitric oxide ions produced during or following photoionization represent the major ions down to about 85 km, with layers of metal ions also being present. Below this height, water cluster ions, $H^+.(H_2O)_n$, predominate. At lower mesospheric levels, negative ions are known to be important but the negative-ion composition has not been established.

1. Introduction

Much of the initiative for studying the ionized and neutral constituents at heights above about 50 km arose from the need to understand the formation of the ionosphere. Rocket-borne mass spectrometer observations (Narcisi 1973) showed the presence of a variety of ions, and a quantitative interpretation of these ions demanded a knowledge of the height distributions of constituents such as water vapour, atomic oxygen and nitric oxide. In the meantime, an understanding of the chemical and physical processes which govern the distributions of both neutral and ionized constituents has become a major field of study in its own right. The more general atmospheric interest in such constituents arises from their role in noctilucent clouds (Witt 1969), airglow emissions (Hunten 1967) and the thermal balance (Crutzen 1970).

The characteristics of the neutral and ionized parts of the atmosphere in the height range 50–130 km are largely determined by the absorption of solar radiations of wavelengths less than about 200 nm, except for those in the 20–80 nm range which are absorbed at greater heights. This is illustrated in figure 1, which shows the heights of unit optical depth for wavelengths up to 310 nm incident vertically, i.e. the heights at which the solar-flux intensities are reduced to e^{-1} of their free space values; these correspond to the levels of maximum absorption.

Also shown in this diagram are the wavelengths corresponding to ionization and dissociation thresholds of important constituents. The dissociation threshold of molecular nitrogen corresponds to a wavelength of 127 nm but the absorption is very weak. For ozone, photodissociation is energetically possible for wavelengths less than 1180 nm, but for the present heights of interest the spectral region below 310 nm is the most effective, producing the first electronically excited states of atomic and molecular oxygen, $O(^1D)$ and $O_2(^1\Delta_g)$. The constituents chiefly responsible for absorption in the different wavelength regions are as shown in figure 1. Absorption by molecular oxygen in the Schumann–Runge ($B^3\Sigma_u^- – X^3\Sigma_g^-$) band system between 175 nm and

205 nm is of particular interest in view of the marked variation of absorption cross section with wavelength and the pronounced changes with temperature (Ackerman *et al.* 1970). Account needs to be taken of these properties of the oxygen cross section in detailed treatments of the photodissociation of nitric oxide, carbon dioxide, and also of water in the lower mesosphere. Radiations capable of ionizing the major constituents are absorbed, in the main, above 95 km but deep windows occur between about 110 and 130 nm, one of which coincides with the strong Lyman-α line at 121.6 nm, permitting the photoionization of $O_2(^1\Delta_g)$ and NO at D-region heights.

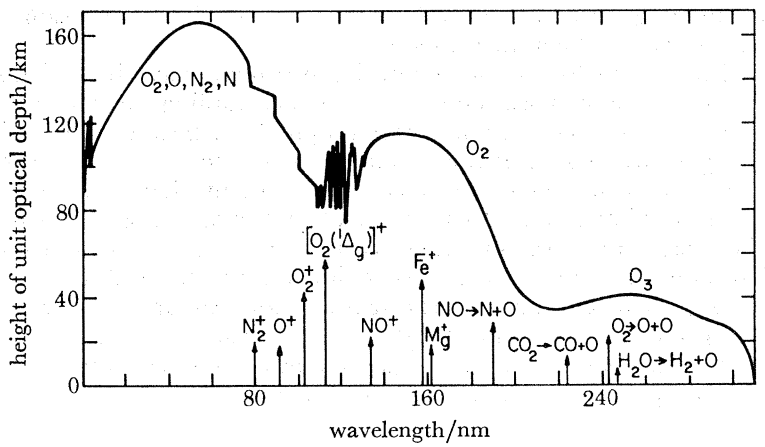

FIGURE 1. The variation with wavelength of the height of unit optical depth for solar radiations incident vertically. The wavelengths corresponding to the ionization and dissociation thresholds of certain constituents are indicated; ionization processes are represented by + sign.

Relatively few measurements of neutral composition have been made in the region between 50 and 130 km and our present knowledge and understanding are based largely on theoretical models. These involve solutions of the continuity equations for individual constituents with account being taken of photodissociation or photoionization and chemical reactions in the production and loss terms. For constituents having long lifetimes, transport processes can seriously influence the spatial variations, and increased attention has been paid in the past decade to the incorporation of such processes in theoretical models. To date, the greatest attention has been paid to vertical diffusion, the effects of both molecular and turbulent diffusion being first examined for molecular and atomc oxygen by Colegrove *et al.* (1965), but subsequently considered in connection with a number of other constituents.

The purpose of the present paper is to describe the available experimental information on the neutral and ion composition in the height range 50–130 km. For the neutral constituents it is convenient to consider in turn oxygen, hydrogen, nitrogen and carbon species. For ionized constituents a subdivision based on height of occurrence is more natural; it is found that above about 90 km the observed ions represent in the main the products of the primary photoionization processes, whereas at lower heights they arise from reactions of these products with molecules. Where possible, the experimentally determined distributions for both neutral and ionized constituents are related to corresponding theoretical predictions.

2. Neutral composition

(a) *Oxygen species*

(i) *Molecular oxygen*

As indicated in figure 1, the atmospheric penetration of solar radiations in the extreme ultraviolet (e.u.v.) wavelength region is controlled by molecular oxygen absorption. Friedman *et al.* (1951) first took advantage of this to estimate molecular oxygen concentrations in the thermosphere from rocket-borne measurements of solar e.u.v. intensities. More recently, this approach has also been used in satellite observations of occultation of the sun by the Earth's limb. The early rocket observations of ultraviolet absorption and of mass spectrometer sampling were reviewed by Offermann (1974). In the meantime, the mass spectrometer technique has been improved by the use of cryogenically cooled sources (Offerman & Tatarczyk 1973), which minimizes the formation of background gases within the source, and also eliminates the shock front ahead of the ion source; measurements with this technique can now be achieved down to 80–90 km.

Rocket-borne measurements of the molecular oxygen height distribution using a Lyman-α sensor (Weeks 1975) and a mass spectrometer (Trinks *et al.* 1978*a*) have shown the presence of wavelike structures in the height region 75–150 km. Measurements of absorption at 145 nm (Higgins & Heroux 1977), referring to the upper part of the height region of interest, indicate increases in molecular oxygen concentration at times of magnetic disturbance which are consistent with previous results derived for greater heights using satellite observations of solar ultraviolet occultation. Recent occultation measurements at more than one wavelength by Garriott *et al.* (1977) have also shown that such increases of molecular oxygen occur near 130 km but not at 100 km. These observations carried out in solar minimum years also revealed a diurnal variation of molecular oxygen near 100 km, the values deduced at sunset being larger than those at sunrise. Corresponding measurements during solar maximum years by Roble & Norton (1972) also provided evidence of a seasonal change, the summer concentrations being three times the corresponding winter values.

(ii) *Atomic oxygen*

Atomic oxygen, $O(^3P)$, is perhaps the most important single neutral constituent in the 50–130 km height range since it plays a central role in the thermal balance of the lower thermosphere, is involved in reactions responsible for a number of airglow emissions, and is an important reactant in both the positive- and negative-ion chemistry. Consequently, with molecular oxygen, it has attracted the greatest attention in neutral-composition measurements in this height range, and a total of five different rocket-borne experiments have been devised for its measurement. The most successful approaches have involved the use of improved mass spectrometers, in which the nature of the ion source has been a major consideration, and ultraviolet lamps for generating the $OI(^3P–^3S_1)$ triplet near 130 nm; the measurement of resonance scattering of this radiation from ambient atoms provides a sufficient dynamic range to cover the concentrations in the 60–140 km height range, while the simultaneous measurement of absorption over a 40 cm path furnishes the absolute calibration (Dickinson *et al.* 1979). The use of a cryogenically cooled ion source in the mass spectrometer (see, for example, Offerman & von Zahn 1971; Trinks *et al.* 1978*a*) has minimized the loss of atomic oxygen at the source walls, and the incorporation of cryogenic pumps (Philbrick *et al.* 1973; Arnold & Krankowsky 1977*a*)

PHILOSOPHICAL TRANSACTIONS OF THE ROYAL SOCIETY A MATHEMATICAL, PHYSICAL & ENGINEERING SCIENCES

has enabled measurements to be extended down to 80 km; for such heights, a suitably shaped sampling cone (Arnold & Krankowsky 1975) has reduced the difficulties associated with the formation of a detached bow shock.

Even with these improvements, the atomic oxygen data available from the use of mass spectrometers are still sparse, but the repeated use of the ultraviolet lamp technique (Dickinson *et al.* 1979) has provided information on the distribution over the 60–140 km height range during a variety of conditions. The curves in figure 2 represent the results of measurements during

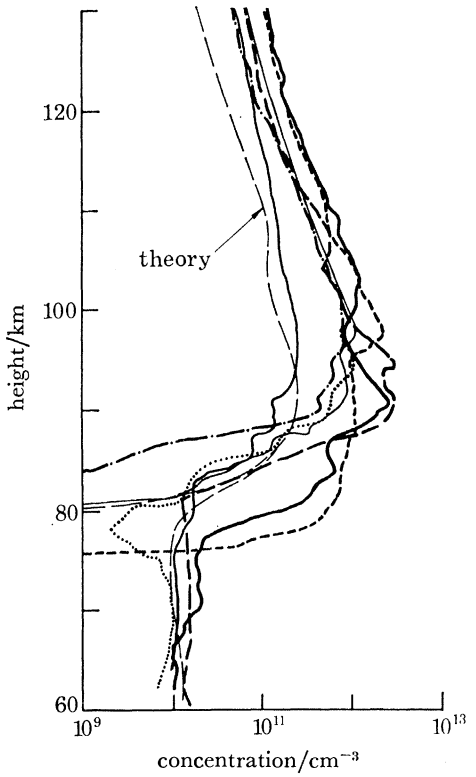

FIGURE 2. Height distributions of atomic oxygen measured at S. Uist, Scotland (Dickinson *et al.* 1979), and deduced using a theoretical model (Thomas & Bowman 1972). The distributions showing decreases to low concentrations below the maxima refer to night-time conditions, and those showing almost constant concentrations below about 77 km refer to daytime; the dotted curve represent measurements during a dawn period.

seven rocket flights at S. Uist, Scotland, during winter and equinox months in the period April 1974–February 1977. Also shown by the labelled curves are the results deduced theoretically for daytime and night-time during equinox months at mid-latitudes (Thomas & Bowman 1972). The predicted disappearance of oxygen atoms at heights below about 81 km between daytime and night-time is reproduced in the measurements, although the actual height at which this change occurs is very variable. From figure 2 it is seen that at heights near and above the maxima in the atomic oxygen distributions the observations show considerably larger concentrations than those predicted theoretically. For these heights the factors determining the atomic oxygen concentrations in the theoretical model are chiefly the solar-flux intensities, particularly in the 130–200 nm wavelength range, and the values of the coefficient representing vertical turbulent diffusion (Lettau 1951; Colegrove *et al.* 1965). The solar-flux

intensities have been the subject of some controversy but the relatively low values of Parkinson & Reeves (1969) adopted in the present theoretical results have been confirmed in more recent results (Delaboudinière *et al.* 1978). A reduction in the values of eddy diffusion coefficient adopted in the theoretical treatment by a factor of 3 or 4 at all heights could be sufficient to reconcile the predicted concentrations with the observations, the reduced values still being within the range suggested by von Zahn (1967) in connection with observations of argon and molecular nitrogen concentrations.

A notable feature of the atomic oxygen distributions in figure 2 is the marked wavelike structure observed at heights above about 80 km; attention has already been drawn to the presence of such structure in corresponding molecular oxygen measurements.

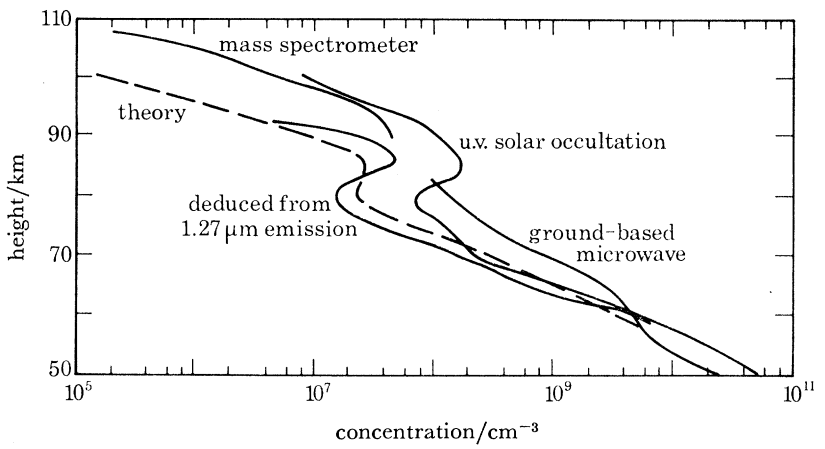

Figure 3. Daytime height distributions of ozone derived from rocket-borne observations of $O_2(a^1\Delta_g–X^3\Sigma_g^-)$ emissions at 1.27 μm (Llewellyn & Witt 1977), of solar ultraviolet occultation (Miller 1976), and of concentrations, with the use of a mass spectrometer (Weeks *et al.* 1978); results deduced from observations of thermal emission at 110.8 GHz are also shown (Penfield *et al.* 1976). A distribution obtained by using a theoretical model (Thomas & Bowman 1972) is included for comparison.

(iii) *Ozone*

The primary interest in ozone at mesospheric heights arises from its role in the excitation of infrared emissions in the airglow and in the negative-ion chemistry. Height distributions measured during daytime using four different techniques are shown in figure 3. The maximum observed near 85 km was first identified by Evans *et al.* (1968) from rocket-borne observations of the (0–0) band emission of $O_2(a\ ^1\Delta_g–X\ ^3\Sigma_g^-)$ at 1.27 μm in the dayglow, on the basis that the excited molecules are produced by the photolysis of ozone by absorption of solar radiation in the Hartley continuum (Vallance Jones & Gattinger 1963). The corresponding profile in figure 3 was derived for daytime by Llewellyn & Witt (1977) from measurements during twilight at Kiruna, Sweden, during March 1975. The solar ultraviolet occultation method takes advantage of the dominant influence of ozone on absorption of radiations of wavelengths above about 220 nm, the distribution shown in figure 3 being measured by Miller (1976). Observation from a satellite of the attenuation of ultraviolet radiations from stellar sources (Hays & Roble 1973) have also shown the presence of the mesospheric maximum in the ozone height distribution. Theoretical studies reproduce this maximum in the distribution, as illustrated by the results of Thomas & Bowman (1972) represented by the broken curve in figure 3; these studies have demonstrated that the distinction and magnitude of this feature depend on

the values of the eddy diffusion coefficient, and for large values of this coefficient it almost disappears.

The mass spectrometer results of Weeks *et al.* (1978) extend to the greatest heights in figure 3 and the microwave measurements from about 82 km downwards refer to measurements of the emission of the 100.8 GHz rotational line by Penfield *et al.* (1976). The latter measurements showed a day-to-night increase in concentration by a factor of about 2 over the 55–80 km height range. Some evidence for such a diurnal change has also been found by Noxon (1975) from an analysis of the difference between the morning and evening twilight enhancements of the (0–1) band of $O_2(b\ ^1\Sigma_g^- - X\ ^3\Sigma_g^-)$ emission at 864 nm, assuming that excitation occurs by energy transfer from $O(^1D)$ atoms produced by ozone photolysis. Such a day-to-night change in ozone concentration is predicted by theoretical models (Thomas & Bowman 1972; Moreels *et al.* 1977).

(iv) $O_2(a\ ^1\Delta_g)$

Apart from their role as the source of the infrared atmospheric system in airglow emissions, $O_2(a\ ^1\Delta_g)$ molecules represent an important ionizable constituent in the D-region and are also involved in the negative-ion chemistry. The height distributions of these excited molecules during daytime and twilight, as deduced from airglow observations, can be understood on the basis of current photochemical models. However, the observed emission intensities at 1.27 μm during night-time are larger than are predicted by these models. It has been usually considered that the recombination of oxygen atoms in the presence of a third body is responsible for these excited molecules at night-time, but the discrepancy between theory and experiment implies that some other mechanism is involved (Moreels *et al.* 1977).

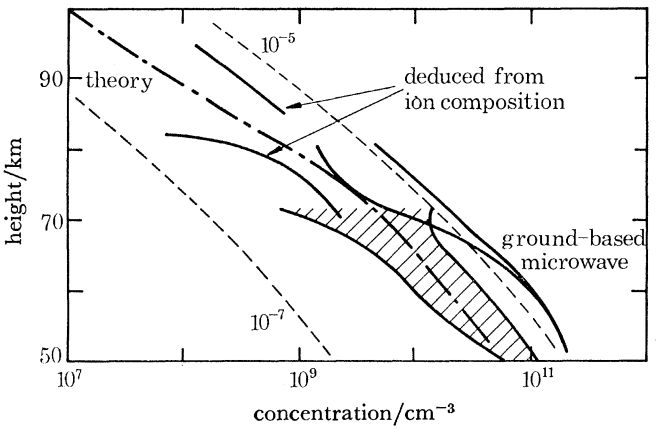

FIGURE 4. Height distributions of water vapour derived from rocket-borne observations of thermal emission in the wing of the 6.3 μm band (Rogers *et al.* 1977) and of ion composition (Swider & Narcisi 1975; Arnold & Krankowsky 1977*b*), and from ground-based observations of thermal emission at 22.2 GHz (Radford *et al.* 1977). Also shown is the distribution deduced by using a theoretical model (Thomas & Bowman 1972), and those corresponding to constant mixing ratios of 10^{-5} and 10^{-7}. Shaded region, rocket-borne infrared.

(*b*) *Hydrogen species*

(i) *Water*

The distribution of water vapour in the mesosphere is of interest in studies of noctilucent clouds, in the quantitative interpretation of complex positive ions observed below 80 km (see § 3*b*), and in considerations of the escape of hydrogen atoms from the upper thermosphere.

The limited information available on the water concentration at mesospheric heights is illustrated in figure 4.

The shaded region refers to estimates derived by Rogers *et al.* (1977) from rocket-borne observations of thermal emission in the long-wavelength wing of the 6.3 μm band, using a liquid helium cooled spectrometer; the range of values shown correspond to the 3σ limits on the radiance measurements. Since collisional deactivation of the $H_2O(010)$ molecule is more rapid than spontaneous emission at heights below about 85 km, the interpretation of the data required information on mesospheric temperatures and concentrations of molecular oxygen, nitrogen and carbon dioxide. From this interpretation Rogers *et al.* suggested that the measurements, which were carried out at Chatanika, Alaska, following an auroral glow, were consistent with a mixing ratio of 3.5 ± 2 parts/10^6 between 49 and 70 km. The second direct estimates shown in figure 4 were derived by Radford *et al.* (1977) from ground-based observation of emission of the line centred at 22.2 GHz, with the use of the 37 m radio telescope at Haystack Observatory, Massachusetts. The height range of the measurements was limited by receiver bandwidth at the lower heights and by the inability to resolve the Doppler-broadened hyperfine components of the line at the upper heights. Radford *et al.* reported errors of $\pm 40\,\%$ in the derived concentrations. It is to be noted that the water concentrations derived were rather larger than those normally expected; the largest value corresponded to a mixing ratio of 15 parts/10^6 at 60 km.

The two other height distributions included in figure 4 were deduced from ion mass spectrometer measurements, on the basis of the known ion chemistry. That shown for the 70–82 km height range is based on data obtained at Fort Churchill, Canada, during a solar proton event (Swider & Narcisi 1975), and that for the 85–95 km range refers to measurements at high-latitude sites in Scandinavia (Arnold & Krankowsky 1977*b*). The two sets of results could have been influenced by fragmentation of weakly bound ambient ions during sampling. It is interesting to note that these two distributions imply quite different conditions of vertical turbulent transport; that of Swider & Narcisi shows little evidence of transport of water molecules from below to replace those destroyed by photodissociation, whereas that of Arnold & Krankowsky indicates a slope similar to those of the lines representing constant mixing of 10^{-5} (10 parts/10^6) and 10^{-7} (0.1 parts/10^6) and, therefore, implies very efficient vertical mixing. The two distributions can be compared in figure 4 with the theoretical results derived by Thomas & Bowman (1972) for intermediate values of eddy diffusion coefficient and a mixing ratio of 3 parts/10^6 at 60 km.

(ii) *Water dissociation products*

According to present ideas, water represents the principal form of hydrogen in the mesosphere, the remainder being present as molecular hydrogen with small amounts of OH, H and HO_2, arising directly or indirectly from water dissociation, and also as methane. At thermospheric heights atomic and, perhaps, molecular hydrogen represent the only significant forms. The only direct measurement of these constituents in the height range of present interest is that of OH by Anderson (1971*a*, *b*) from rocket-borne observations of resonant scattering of the (0–0) band of $OH(A\,^2\Sigma–X\,^2\Pi)$ at 306.4 nm during evening twilight conditions. The local concentrations deduced: 4.4×10^6 cm^{-3} at 50 km, 5.5×10^6 cm^{-3} at 60 km, and 3.5×10^6 cm^{-3} at 70 km are reasonably consistent with values predicted theoretically (Thomas & Bowman 1972; Moreels *et al.* 1977).

Estimates of hydrogen atom concentrations have been made in the interpretation of airglow emission. Evans & Llewellyn (1973) analysed simultaneous measurements of the oxygen infrared atmospheric band and of hydroxyl emissions to deduce, first, the height distribution of ozone and subsequently that of atomic hydrogen, on the basis that the reaction of these two constituents gives rise to the vibrationally excited hydroxyl radicals and, hence, the hydroxyl emissions. These results showed an increase in atomic hydrogen concentration from 10^6 cm^{-3} near 60 km to 3×10^7 cm^{-3} between 80 and 90 km, with values of 10^7 cm^{-3} near 100 km. Noxon (1975) also suggested an upper limit of 8×10^6 cm^{-3} for the atomic hydrogen concentration near 100 km during night-time, to permit the increase of ozone required for the dawn enhancement of the (0–1) band of the atmospheric system of molecular oxygen (see § 2*a* (iii)). These two sets of results imply water mixing ratios much smaller than the 3 parts/10^6 assumed at 60 km in the theoretical curve of figure 4.

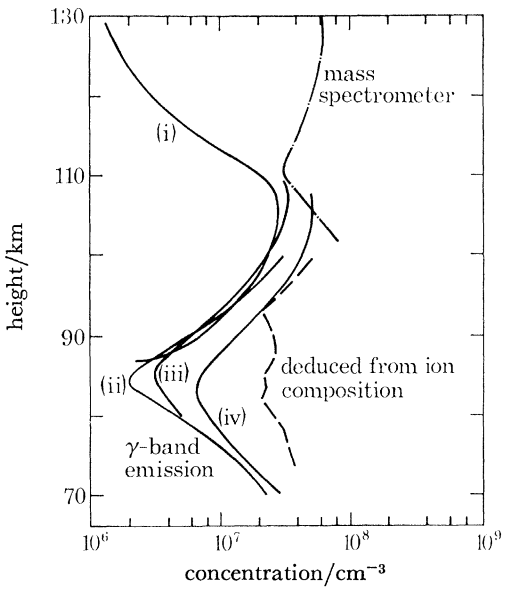

FIGURE 5. Height distributions of nitric oxide derived from rocket-borne observations of the γ-band fluorescence in the dayglow: (i) Tohmatsu & Iwagami (1976), (ii) Baker *et al.* (1977), (iii) Tohmatsu & Iwagami (1975), (iv) Meira (1971); of concentrations with the use of a mass spectrometer (Trinks *et al.* 1978*b*); and of ion composition during a disturbed winter day (Arnold & Krankowsky 1977*a*).

(*c*) *Nitrogen species*

Interest in the nitrogen constituents in the height range of interest has been inspired in part by the importance of nitric oxide in the formation of the ionospheric D-region and as a charge-transfer agent in the E-region. Studies of the other important form of nitrogen, N(^{4}S), at these heights of interest have been limited to theoretical models, although a concentration of 1.9×10^7 cm^{-3} has been deduced by Feldman & Takacs (1974) from the interpretation of twilight airglow observations. Almost all measurements of the nitric oxide distribution in the mesosphere and lower thermosphere have been based on observations of the γ-band fluorescence in the dayglow, after Barth (1964); the (1–0) and (2–0) bands at 214.9 nm and 204.7 nm have generally been used. At mesospheric heights, the need to remove background radiation due to Rayleigh scattering is a major complication. This component was previously deduced from atmospheric density measurements and the resultant small γ-band column emission rates showed large

uncertainties; differentiation of the column rates provided the volume emission rates and, hence, the nitric oxide concentrations. In a development introduced by Tohmatsu & Iwagami (1975), an ultraviolet photometer coupled with a nitric oxide gas-filled absorption cell enables more accurate corrections for the Rayleigh-scattered background radiation to be made and thereby furnishes improved measurements of the dayglow emission; the cell is placed cyclically in the optical path and serves as a rejection filter for the gamma bands.

Figure 5 shows four height distributions of nitric oxide deduced from γ-band observations. Curves (i), (ii), and (iii) were derived from measurements using a nitric oxide filled cell; curve (i) extending from 87 to 130 km is based on measurements of Tohmatsu & Iwagami (1976) in early morning at equatorial latitudes; curve (ii) represents the results of Baker *et al.* (1977) near sunset at mid-latitudes; and curve (iii) was derived for sunset conditions at mid-latitudes by Tohmatsu & Iwagami (1975). The fourth set of results based on γ-band emission measurements, curve (iv) in figure 5, represents the earlier measurement of Meira (1971) near noon at mid-latitudes, and refers to a disturbed winter day (Geller & Sechrist 1971). In all these distributions deduced from γ-band emissions, account has been taken of the recent revision of the emission rate factor (Cravens 1977). Even larger increases in nitric oxide concentrations at mid-latitudes during disturbed winter conditions than those implied by curve (iv) are illustrated by the distribution represented by the broken curve in figure 5. This was deduced from ion-composition measurements carried out during an anomalous winter day in Spain by Arnold & Krankowsky (1977*a*). It is believed that such enhancements in nitric oxide concentrations contribute to the increased electron concentrations which give rise to anomalously high radio-wave absorption on such winter days.

The large concentrations in the lower thermosphere indicated by the mass-spectrometer measurements of Trinks *et al.* (1978*b*) for mid-afternoon at mid-latitudes, figure 5, are supported by simultaneous measurements of the (1–0) band. On this basis, it appears that the differences between the two distributions in the height range 110–130 km in figure 5 cannot be attributed to differences in the experimental techniques adopted. It seems likely that this difference arises in part out of the different local times of measurement, as expected from the theoretical results of Ogawa & Kondo (1977). These workers draw attention to the influence at the heights of interest of nitric oxide transported from upper thermospheric levels where the production from reaction of $N(^4S)$ atoms with oxygen molecules is very dependent on temperature and, hence, on local time. For heights below 100 km the main uncertainty in the theoretical understanding is in the vertical transport but the quantum yield of $N(^2D)$ atoms from various reactions is also relevant since at these heights nitric oxide is chiefly produced by the reaction of these excited atoms with oxygen molecules.

The variability of the nitric oxide concentrations indicated in figure 5 has been examined for lower thermospheric heights by satellite-borne measurements using the γ-band fluorescence technique; these measurements refer to heights above 90 km where the background due to Rayleigh scattering is small. The nadir-viewing experiment on OGO 4 satellite provided measurements of the vertical column density of nitric oxide above the shadow line at twilight; with this experiment Rusch & Barth (1975) found highly variable quantities of nitric oxide at latitudes above 60° N and Gérard & Barth (1977) observed a factor of 4 enhancement at high latitudes during a magnetic storm, the concentration at 110 km reaching a value of 4×10^8 cm^{-3}. More recently, the limb-scanning experiment on Atmospheric Explorer C satellite has provided information on the global morphology of nitric oxide at 105 km, including the effects of

magnetic activity (Cravens & Stewart 1978), and has also demonstrated diurnal and seasonal variations at low latitudes (Stewart & Cravens 1978). The results show concentrations of 4×10^7 cm^{-3} to 6×10^7 cm^{-3} at high latitudes, up to 68° N, with considerable variability; near the equator the concentrations are nearer 2×10^7 cm^{-3} and show little change with longitude or magnetic activity. Also, at low latitudes, the concentrations show an increase from about 10^7 cm^{-3} at sunrise to about 2×10^7 cm^{-3} during the afternoon, followed by a reduction towards sunset; an asymmetry is observed in the nitric oxide distribution about the equator, except during equinox periods, the concentrations being larger on the summer than winter side. No detailed comparison with theory is possible but Stewart & Cravens (1978) deduce that the diurnal changes are consistent with a chemical loss of nitric oxide by reaction with ambient nitrogen atoms, a daytime atomic concentration of 10^7 cm^{-3} being required, which can be compared with the value of 1.9×10^7 cm^{-3} reported previously by Feldman & Takacs (1974).

(*d*) *The carbon species*

The main carbon constituent at 50–130 km is carbon dioxide, although on the basis of theoretical models the monoxide is expected to show comparable concentrations near the upper boundary of this height range (Wofsy *et al.* 1972; Shimazaki & Cadle 1973). The carbon dioxide is of interest primarily because of its role in the thermal balance of the mesosphere and lower thermosphere, and because of its involvement in both the positive and negative-ion chemistry of the D-region.

The measurement of the height distribution of carbon dioxide by mass spectrometer techniques was facilitated by the inclusion of cryogenically cooled ion sources (Offermann & Tatarczyk 1973); these serve to suppress reactions involving oxygen, whose products obscured the carbon dioxide within earlier forms of ion sources. Night-time measurements by Scholz & Offermann (1974) and others showed complete mixing of the constituent up to the turbopause, with a mixing ratio similar to that in the troposphere, i.e. 3×10^{-4}. At greater heights the distribution corresponded to that of diffusive equilibrium. Recently, a similar mass spectrometer experiment successfully measured the carbon dioxide concentrations over the height range 90–150 km during daytime (Trinks & Fricke 1978). The results again showed that below the turbopause the mixing ratio corresponded to that at tropospheric heights but at greater heights the decrease with height was more rapid than that expected for diffusive equilibrium. This is attributed mainly to photolysis up to about 115–120 km, with the production of carbon monoxide, and a reaction with O^+ ions at greater heights with unspecified products. Such photolysis of carbon dioxide by the Schumann–Runge bands is believed to be the main source of carbon monoxide in the mesosphere and upper stratosphere, the dissociation by the Schumann–Runge continuum being more important in the lower thermosphere. Theoretical models incorporating eddy diffusion have predicted the height distribution of carbon monoxide in the mesosphere (Hays & Olivero 1970; Wofsy *et al.* 1972), and these have been considered by Waters *et al.* (1976) in their interpretation of ground-based measurements of the absorption of the carbon monoxide rotational line at 115.3 GHz in the solar spectrum to yield the height distribution of this constituent. The results obtained were consistent with a mixing ratio of about 0.1 parts/10^6 near 50 km increasing to about 10 parts/10^6 near 78 km, and a constant value of about 40 parts/10^6 above 100 km.

3. Ion composition

(*a*) *Upper mesosphere and lower thermosphere*

Measurements of ion composition at heights between about 90 km and 130 km have been chiefly obtained by rocket-borne magnetic and quadrupole mass spectrometers. The results of several measurements (Narcisi 1973) have shown that NO^+ and O_2^+ are the dominant ions during daytime, their concentrations being comparable. At night the relative proportion of NO^+ increases, its concentration being about an order of magnitude greater than that of O_2^+.

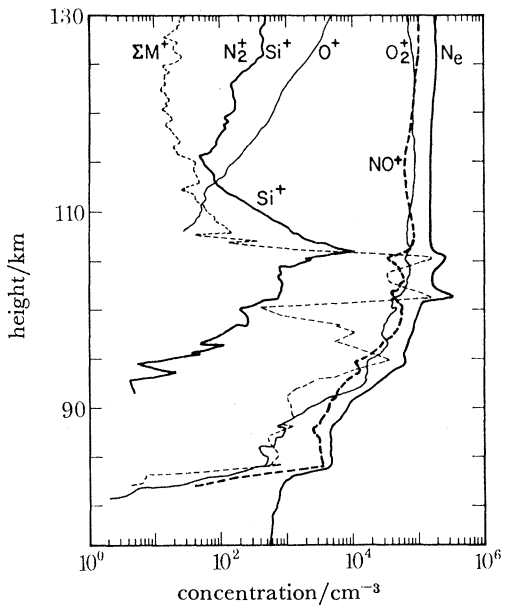

Figure 6. The positive-ion composition and height distributions of total metal-ion and electron concentrations, as derived from rocket-borne mass spectrometer, probe, and radio-propagation measurements (Herrmann *et al.* 1978) at Wallops Island in daytime during August 1976.

Typical daytime results for these ions are shown in figure 6 and are derived from measurements with a magnetic type mass spectrometer by Herrmann *et al.* (1978). Also shown are the height variations of total metal-ion concentrations, ΣM^+. The electron concentrations, N_e, were deduced from probe and propagation experiments. The observations of metal ions, with Mg^+ and Fe^+ being predominant, in the region 85–120 km is a common finding of mass spectrometer observations; the layer with a peak near 94–95 km is a permanent feature of the lower ionospheres, but the upper layer is more intermittent.

It is usually considered that the occurrence of O_2^+ and NO^+ ions is a well understood characteristic of the E-region. Only a few chemical reactions control the relative proportions of NO^+, O_2^+, O^+ and N_2^+ ions but these reactions involve the minor neutral constituents O, NO, N, as well as the major constituents O_2 and N_2, and a knowledge of the neutral composition is, therefore, essential. In view of the marked temperature gradient in this height region, data on the temperature dependence of chemical rate coefficients is also an important requirement. Attention has been paid to this temperature dependence in laboratory measurements over the past decade and information is also being obtained from analyses of Atmospheric Explorer

satellite data for greater heights (Torr & Torr 1978). For night-time conditions, a detailed understanding of the ion-composition measurements requires information on the production of ionization by scattered Lyman-α and Lyman-β radiations. Furthermore, with the longer lifetimes for ions resulting from the smaller ionization densities, account needs to be taken of the movements of ionization in the upper part of the height region under consideration (Strobel *et al.* 1974).

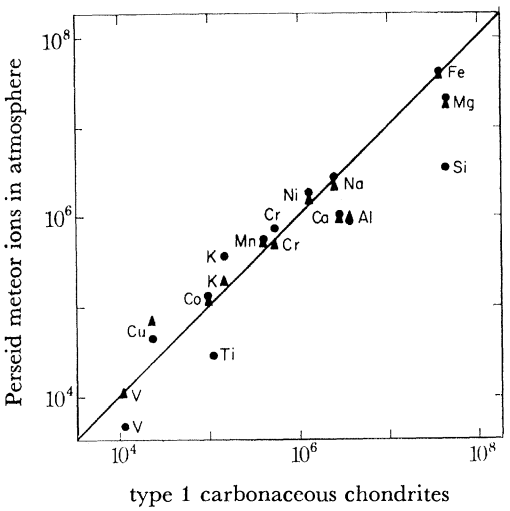

FIGURE 7. A comparison of the relative concentrations of metal ions observed between 91 and 107.5 km and of metal atoms in carbonaceous chondrites, normalized to the values for iron (Herrmann *et al.* 1978). ●, 99–107.5 km; ▲, 91–99 km.

The observations that the metal-ion concentrations are enhanced during periods of meteoric activity (Narcisi 1968; Goldberg & Aikin 1973) have suggested a meteoric source for the corresponding metal atoms. Support for this suggestion has been found in the agreement between the relative abundance of observed ions and of metal atoms in chondrite meteorites, first noted by Goldberg & Aikin (1973). In this connection, the relative concentrations of metal ions observed during the measurements of figure 6, which were carried out 12 h after the Perseid meteor shower, have been compared by Herrmann *et al.* (1978) with the metal-atom concentrations in carbonaceous chondrites, as shown in figure 7; here the values were normalized to those of iron. It is seen that for elements such as Ni, Cr, Co, Mn and Na the agreement is very good, but marked discrepancies can be seen for Ti and Si. The importance of a meteor source for alkali metals has also been demonstrated in some measurements of the column densities of sodium and potassium atoms in the height ranges 80–100 km from the resonance scattering of suitably tuned ground-based laser beams (Megie *et al.* 1978). However, it is suggested that during winter months the relative concentrations of these elements are no longer consistent with a meteoric source and a possible contribution from sea spray is invoked.

Consideration of the cross sections for collisions at high energies has suggested that the production of metal ions during meteor ablation is relatively unimportant. Instead, a large proportion of the observed ions is believed to arise from photoionization or charge-transfer processes. The ionization thresholds for iron and magnesium correspond to wavelengths of 157.5 nm and 162.2 nm, respectively, and, as seen from figure 1, these do not penetrate below 100 km. However, because of the relatively low energies corresponding to these thresholds,

and still smaller values for sodium and others atoms, charge transfer can occur even with NO^+ ions. The direct loss of the metal ions by radiative recombination is slow and it seems likely that transport to lower levels followed by three-body processes are chiefly responsible for their disappearance.

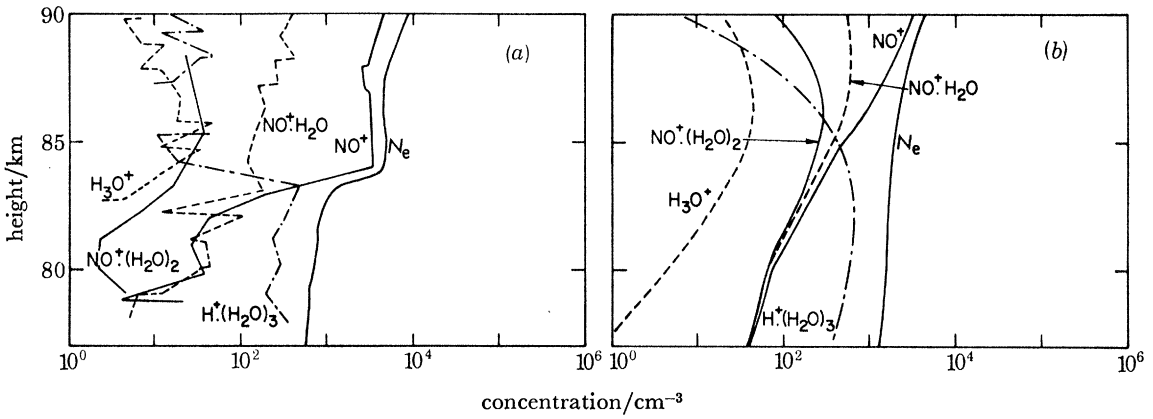

FIGURE 8. A comparison of (*a*) a simplified version of the ion composition measured in daytime using a rocket-borne mass spectrometer at Wallops Island during August 1976 (Kopp *et al.* 1978) and (*b*) the ion composition predicted for summer daytime conditions by using a theoretical model in which NO^+ represents the precursor of water cluster ions (Thomas 1976).

(*b*) *Middle and lower mesosphere*

(i) *Positive ions*

Rocket-borne measurements with quadrupole and magnetic mass spectrometers, incorporating suitable pumping arrangements, carried out since 1963 at a number of sites have shown that under normal conditions ions of the type $H^+.(H^2O)_n$ dominate the positive-ion composition below about 83 km in daytime, and below about 86 km during twilight or night-time. The majority of early measurements showed $H^+.(H_2O)_2$ as the dominant cluster ion with significant concentrations of H_3O^+ and $H^+.(H_2O)_3$ also being present. There is, however, some doubt whether these measurements represented ambient conditions since fragmentation of complex weakly bound ions could occur through thermodynamic break-up because of increased temperatures at the shock layer associated with the supersonic velocity of the rocket, or through collisions resulting from the draw-in electric fields. To overcome these effects, modified geometries of the sampling region have been introduced and lower attracting potentials (Arnold & Krankowsky 1975; Kopp *et al.* 1978). With these improvements, higher-order cluster ions have been customarily observed.

The main features of the results during a daytime flight of the magnetic mass spectrometer are shown in figure 8*a*. This represents a simplified version of the observations presented by Kopp *et al.* (1978); thus the O_2^+ ion distribution is not shown and that of $H^+.(H_2O)_4$, which is almost identical with that of $H^+.(H_2O)_3$, is also omitted. Similar results have been found on a number of occasions using a quadrupole mass spectrometer experiment (Arnold & Krankowsky 1977*a*).

The early measurement of these water cluster ions by Narcisi & Bailey (1965) was quite unexpected on the basis of the prevailing ideas concerning the formation of the D-region (Nicolet & Aikin 1960); NO^+ and O_2^+, produced both by photoionization and by ion–molecule reactions were predicted as the dominant ions. Although a reaction scheme for the formation of

cluster ions from O_2^+ ions was formulated on the basis of laboratory measurements, the supply of O_2^+ ions from the photoionization of $O_2(^1\Delta_g)$ (Huffman *et al.* 1971) is believed to be too small to be significant. Instead, NO^+ is now believed to be the precursor of water cluster ions under normal conditions. Reactions involving the successive hydration by three-body attachment of water molecules to produce $NO^+.(H_2O)_3$ followed by the formation of $H^+.(H_2O)_3$, were first proposed by Fehsenfeld & Ferguson (1969). The inclusion of more rapid hydration processes involving weakly-bound intermediate ions, such as $NO^+.CO_2$ and $NO^+.N_2$, has helped to formulate a reaction scheme for the formation of water cluster ions from NO^+ ions. One aspect of this scheme, which arises from the temperature dependence of the three-body processes giving rise to these intermediate ions and of the collisional dissociation of these ions, is a marked temperature dependence expected for the ion composition of the ionospheric D-region. Recent calculations based on this scheme have shown that the main features of the ion composition are reproduced. This is illustrated in figure 8*b*, which shows results of calculations for summer conditions, as described by Thomas (1976). It is seen that the relative concentrations of different ion species are similar to those in the experimental results, presented in figure 8*a*. By suitable choice of the height distribution of nitric oxide concentration, and of temperature, it would be possible to reproduce the general forms of the ion distributions. A notable difference in figure 8*a*, *b* is that the theoretically predicted concentrations of $NO^+.(H_2O)_2$, and to a lesser extent of $NO^+.H_2O$, are substantially larger than those actually observed. Reid (1977) has suggested that this discrepancy between theory and observation arises because of dissociation of the NO^+ hydrates during mass spectrometer sampling. Alternatively, Charkrabarty *et al.* (1978) have invoked collisional dissociation of the first and second hydrates of NO^+, and have adopted values of rate coefficients to ensure agreement between theoretical results and observations. However, there is no supporting evidence for such values from laboratory investigations.

(ii) *Negative ions*

It is well known that the relatively large atmospheric pressures encountered at D-region heights permit the formation of negative ions by the three-body attachment of electrons to neutral atoms and molecules. Early laboratory measurements showed that such attachment occurs rapidly for molecular oxygen, but more recent studies have revealed that the O_2^- ions take part in a complicated sequence of reactions involving the neutral constituents O_3, CO_2, NO, NO_2, and H_2O.

The information on negative-ion composition, derived from two sets of mass spectrometer measurements, has shown serious discrepancies, as illustrated in Figure 9*a*, *b*. The results of figures 9*a* refer to measurement by Arnold *et al.* (1971) during weak auroral conditions at high latitudes, and those of figure 9*b* represent the measurements of Narcisi *et al.* (1972) carried out at middle latitudes near totality of a solar eclipse. Figure 9*a* indicates that CO_3^- was the dominant ion present, significant concentrations of HCO_3^- and NO_3^- were present between about 70 and 80 km, and substantial concentrations of Cl^- ions, of isotopic masses 35^- and 37^-, were also observed. In figure 9*b* the negative-ion composition is dominated by cluster ions of masses corresponding to $NO_3^-.(H_2O)_n$, with possible admixtures of $CO_3^-.(H_2O)_n$, where n = 0–5, and a layer of ions of masses in excess of 150^- was also observed near 88 km.

Neither of these sets of mass spectrometer observations are consistent with what is predicted from theoretical models based on laboratory measurements of negative-ion reactions. However, the relative concentrations of negative and positive ions, measured during the total-ion mode

of operation of mass spectrometers and with electrostatic probes for total positive-ion concentrations, show good agreement with theoretical predictions. This is illustrated in figure 10, which compares the results of daytime measurements during winter at two mid-latitude sites (Arnold & Krankowsky 1977*a*, 1978) with results derived from a theoretical model (Thomas *et al.* 1973). These height variations indicate that free electrons are the dominant negatively charged species at heights above about 70 km.

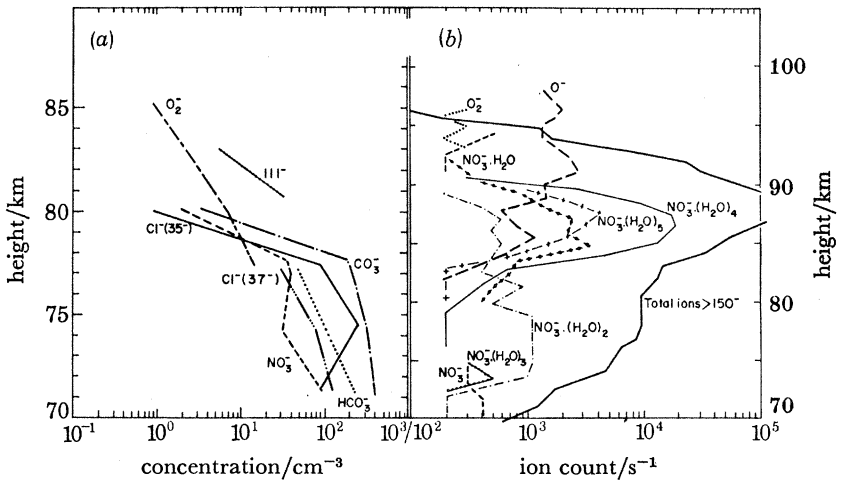

FIGURE 9. The negative-ion composition of the D-region as measured by rocket-borne mass spectrometer: (*a*) Arnold *et al.* (1971); (*b*) Narcisi *et al.* (1972).

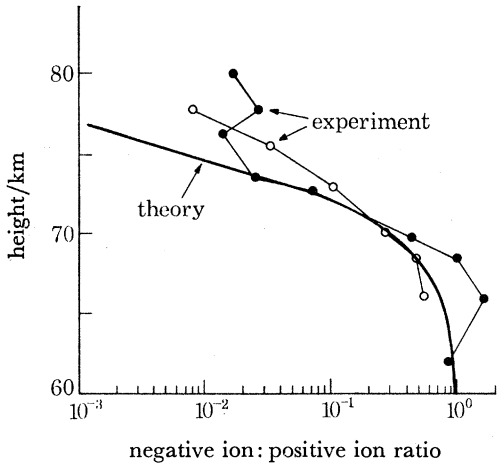

FIGURE 10. A comparison of the ratios of negative-ion to positive-ion concentrations, as deduced from rocket-borne measurements with mass spectrometers and probes (Arnold & Krankowsky 1977*a*, 1978), with those derived using a theoretical model (Thomas *et al.* 1973).

4. CONCLUSIONS

Measurements of neutral and ionized constituents in the mesosphere and lower thermosphere have been limited by the fact that *in situ* sampling can, in general, be achieved only from rockets. Furthermore, remote-sensing measurements of minor neutral constituents based on optical techniques have encountered serious difficulties, especially from Rayleigh scattering at

mesospheric heights. As a consequence, most investigations involving a knowledge of the neutral or ionized composition at these heights have relied heavily on theoretical models. In this connection, the agreement found between the main features of the theoretical predictions and the limited experimental data acquired in recent years (see §§ 3 and 4) is encouraging.

The height distributions measured for certain constituents, such as those for atomic oxygen and nitric oxide in figures 2 and 5, respectively, have indicated considerable variability. To understand such variability, measurements with a particular technique need to be extended in time and in geographic coverage, as illustrated by the satellite-borne measurements in the lower thermosphere of molecular oxygen from observations of solar e.u.v. occultation (see § 2*a*(i)) and of nitric oxide from observations of the γ-band fluorescence in the dayglow (see § 2*c*). Similar observations of thermal emissions and solar occultation in the infrared and microwave spectral regions hold considerable promise of measuring several minor neutral constituents in the heights of present interest on a worldwide basis.

Improved information on the distributions of minor neutral constituents, such as atomic oxygen and nitric oxide, will help resolve some of the uncertainties in the current understanding of the ionospheric D- and E-regions. It has become clear that the neutral and ionized chemistries cannot be realistically separated. For instance, nitric oxide represents a critical constituent in the ion chemistry of the D- and E-regions but its production is itself dependent on the formation of $N(^2D)$ atoms, largely during processes involving NO^+ and N_2^+ ions. The need for coordinated measurements of neutral and ion composition is, therefore, indicated. Such measurements of neutral and positive-ion composition will benefit from recent developments in mass spectrometer techniques but, to date, these have not been successful in establishing the ambient negative-ion composition of the lower D-region.

References (Thomas)

Ackerman, M., Biaume, F. & Kockarts, G. 1970 *Planet. Space Sci.* **18**, 1639–1651.

Anderson, J. G. 1971*a* *J. geophys. Res.* **76**, 4634–4652.

Anderson, J. G. 1971*b* *J. geophys. Res.* **76**, 7820–7824.

Arnold, F., Kissel, J., Krankowsky, D., Wieder, H. & Zahringer, J. 1971 *J. atmos. terr. Phys.* **33**, 1169–1175.

Arnold, F. & Krankowsky, D. 1975 *Proc. Int. Symp. on Solar Terrestrial Physics*, Sao Paulo, Brazil, vol. 3, pp. 30–50. May 1974.

Arnold, F. & Krankowsky, D. 1977*a* *Dynamical and chemical coupling between the neutral and ionized atmosphere* (ed. B. Grandal & J. A. Holtet), pp. 93–127. Dordrecht: D. Reidel.

Arnold, F. & Krankowsky, D. 1977*b* *Nature, Lond.* **268**, 218–219.

Arnold, F. & Krankowsky, D. 1978 *Report of Max-Planck-Institute for Nuclear Physics*, Heidelberg, F.R. Germany, V9.

Baker, K. D., Nagy, A. F., Olsen, R. O., Oran, E. S., Randhawa, J., Strobel, D. F. & Tohmatsu, T. 1977 *J. geophys. Res.* **82**, 3281–3286.

Barth, C. A. 1964 *J. geophys. Res.* **69**, 3301–3303.

Chakrabarty, D. K., Chakrabarty, P. & Witt, G. 1978 *J. atmos. terr. Phys.* **40**, 437–442.

Colegrove, F. D., Hanson, W. B. & Johnson, F. S. 1965 *J. geophys. Res.* **70**, 4931–4941.

Cravens, T. E. 1977 *Planet. Space Sci.* **25**, 369–372.

Cravens, T. E. & Stewart, A. I. 1978 *J. geophys. Res.* **83**, 2446–2452.

Crutzen, P. 1970 *Q. Jl R. met. Soc.* **96**, 767–769.

Delaboudinière, J. P., Donnelly, R. F., Hinteregger, A. E., Schmidtke, G. & Simon, P. C. 1978 *Intercomparison/compilation of relevant solar flux data related to aeronomy, COSPAR, Technique Manual* 7.

Dickinson, P. H. G., Bain, W. C., Thomas, L., Williams, E. R., Jenkins, D. B. & Twiddy, N. D. 1979 *Proc. R. Soc. Lond.* A (In the press).

Evans, W. F. J., Hunten, D. M., Llewellyn, E. J. & Vallance Jones, A. 1968 *J. geophys. Res.* **73**, 2885–2896.

Evans, W. F. J. & Llewellyn, E. J. 1973 *J. geophys. Res.* **78**, 323–326.

Fehsenfeld, F. C. & Ferguson, E. E. 1969 *J. geophys. Res.* **74**, 2217–2222.

PHILOSOPHICAL TRANSACTIONS OF THE ROYAL SOCIETY A MATHEMATICAL, PHYSICAL & ENGINEERING SCIENCES

Feldman, P. D. & Takacs, P. Z. 1974 *Geophys. Res. Lett.* **1**, 169–171.
Friedman, H., Lichtman, S. W. & Byram, E. T. 1951 *Phys. Rev.* **83**, 1025–1030.
Garriott, O. K., Norton, R. B. & Timothy, T. G. 1977 *J. geophys. Res.* **82**, 4973–4982.
Geller, M. A. & Sechrist, C. F. 1971 *J. atmos. terr. Phys.* **33**, 1027–1040.
Gérard, J. C. & Barth, C. A. 1977 *J. geophys. Res.* **82**, 674–680.
Goldberg, R. A. & Aikin, A. C. 1973 *Science, N.Y.* **180**, 294–296.
Hays, P. B. & Olivero, J. J. 1970 *Planet. Space Sci.* **18**, 1729–1733.
Hays, P. B. & Roble, R. G. 1973 *Planet. Space Sci.* **21**, 273–279.
Herrmann, U., Eberhardt, P., Hidalgo, M. A., Kopp, E. & Smith, L. G. 1978 *Space research* XVIII (ed. M. J. Rycroft), pp. 249–252. Oxford: Pergamon.
Higgins, J. E. & Heroux, L. 1977 *J. geophys. Res.* **82**, 3295–3298.
Huffman, R. E., Paulsen, D. E., Larrabee, J. C. & Cairns, R. B. 1971 *J. geophys. Res.* **76**, 1028–1038.
Hunten, D. M. 1967 *Space Sci. Rev.* **6**, 493–573.
Kopp, E., Eberhardt, P. & Herrmann, U. 1978 *Space research* XVIII (ed. M. J. Rycroft), pp. 245–248. Oxford: Pergamon.
Lettau, H. 1951 *Compendium of meteorology* (ed. T. F. Malone), pp. 320–333. Boston, Mass.: American Meteorological Society.
Llewellyn, E. J. & Witt, G. 1977 *Planet. Space Sci.* **25**, 165–172.
Megie, G., Bos, F., Blamont, J. E. & Chanin, M. L. 1978 *Planet. Space Sci.* **26**, 27–35.
Meira, L. G. 1971 *J. geophys.* **76**, 202–212.
Miller, D. E. 1976 Reported by Llewellyn & Witt (1977).
Moreels, G., Megie, G., Vallence Jones, A. & Gattinger, R. L. 1977 *J. atmos. terr. Phys.* **39**, 551–570.
Narcisi, R. S. 1968 *Space research* VIII (ed. A. P. Mitra, L. G. Jacchia & W. S. Newman), pp. 360–369. Amsterdam: North-Holland.
Narcisi, R. S. 1973 *Physics and chemistry of upper atmosphere* (ed. B. M. McCormac), pp. 171–183. Dordrecht: D. Reidel.
Narcisi, R. S. & Bailey, A. D. 1965 *J. geophys. Res.* **70**, 3687–3700.
Narcisi, R. S., Bailey, A. D., Wlodyka, L. E. & Philbrick, C. R. 1972 *J. atmos. terr. Phys.* **34**, 647–658.
Nicolet, M. & Aikin, A. C. 1960 *J. geophys. Res.* **65**, 1469–1483.
Noxon, J. F. 1975 *J. geophys. Res.* **80**, 1370–1373.
Offermann, D. 1974 *J. geophys. Res.* **79**, 4281–4293.
Offerman, D. & Tatarczyk, H. 1973 *Rev. scient. Instrum.* **44**, 1569–1572.
Offerman, D. & von Zahn, U. 1971 *J. geophys. Res.* **76**, 2520–2522.
Ogawa, T. & Kondo, Y. 1977 *Planet. Space Sci.* **25**, 735–742.
Parkinson, W. H. & Reeves, E. M. 1969 *Solar Phys.* **10**, 342–347.
Penfield, H., Litvak, M. M., Gottlieb, C. A. & Lilley, A. E. 1976 *J. geophys. Res.* **81**, 6115–6120.
Philbrick, C. R., Faucher, G. A. & Trzcinski, E. 1973 *Space research* XIII (ed. M. J. Rycroft & S. K. Runcorn), pp. 255–160. Berlin: Akademie-Verlag.
Radford, H. E., Litvak, M. M., Gottlieb, C. A., Gottlieb, E. W., Rosenthal, S. K. & Lilley, A. E. 1977 *J. geophys. Res.* **82**, 472–478.
Reid, G. C. 1977 *Planet Space Sci.* **25**, 275–290.
Roble, R. G. & Norton, R. B. 1972 *J. geophys. Res.* **77**, 3524–3533.
Rogers, J. W., Stair, A. T., Degges, T. C., Wyatt, C. L. & Baker, D. J. 1977 *Geophys. Res. Lett.* **4**, 366–368.
Rusch, D. W. & Barth, C. A. 1975 *J. geophys. Res.* **80**, 3719–3721.
Scholz, T. G. & Offermann, D. 1974 *J. geophys. Res.* **79**, 307–310.
Shimazaki, T. & Cadle, R. D. 1973 *J. geophys. Res.* **78**, 5352–5361.
Stewart, A. I. & Cravens, T. E. 1978 *J. geophys. Res.* **83**, 2453–2456.
Strobel, D. F., Young, T. R., Meier, R. R., Coffey, T. P. & Ali, A. W. 1974 *J. geophys. Res.* **79**, 3171–3178.
Swider, W. & Narcisi, R. S. 1975 *J. geophys. Res.* **80**, 655–664.
Thomas, L. 1976 *J. atmos. terr. Phys.* **34**, 1345–1350.
Thomas, L. & Bowman, M. R. 1972 *J. atmos. terr. Phys.* **34**, 1843–1858.
Thomas, L., Gondhalekar, P. M. & Bowman, M. R. 1973 *J. atmos. terr. Phys.* **35**, 397–404.
Tohmatsu, T. & Iwagami, N. 1975 *Space research* XV (ed. M. J. Rycroft), pp. 241–245. Berlin: Akademie-Verlag.
Tohmatsu, T. & Iwagami, N. 1976 *J. Geomagn. Geoelect., Kyoto* **28**, 343–358.
Torr, T. G. & Torr, M. R. 1978 *Rev. Geophys. Space Phys.* **16**, 327–340.
Trinks, H. & Fricke, K. H. 1978 *J. geophys. Res.* **83**, 3883–3886.
Trinks, H., Offermann, D., von Zahn, U. & Steinhauer, C. 1978*a* *J. geophys. Res.* **83**, 2169–2176.
Trinks, H., von Zahn, U., Barth, C. A. & Kelly, K. K. 1978*b* *J. geophys. Res.* **83**, 203–206.
Vallance Jones, A. & Gattinger, R. L. 1963 *Planet. Space Sci.* **11**, 961–974.
Waters, J. W., Wilson, W. J. & Shimabukuro, F. I. 1976 *Science, N.Y.* **191**, 1174–1175.
Weeks, L. H. 1975 *J. geophys. Res.* **80**, 3655–3660.
Weeks, L. H., Good, R. E., Randhawa, J. S. & Trinks, H. 1978 *J. geophys. Res.* **83**, 978–982.

PHILOSOPHICAL TRANSACTIONS OF THE ROYAL SOCIETY A MATHEMATICAL, PHYSICAL & ENGINEERING SCIENCES

Witt, G. 1969 *Space research* IX (ed. K. S. W. Champion, P. A. Smith & R. L. Smith-Rose), pp. 157–169. Amsterdam: North-Holland.
Wofsy, S. C., McConnell, J. C. & McElroy, M. B. 1972 *J. geophys. Res.* **77**, 4477–4493.
von Zahn, U. 1967 *J. geophys. Res.* **72**, 5933–5937.

PHILOSOPHICAL TRANSACTIONS OF THE ROYAL SOCIETY A MATHEMATICAL, PHYSICAL & ENGINEERING SCIENCES